Lung X-Ray Segmentation using Quadrant-Based Tracing Method

Muhammad Qurhanul Rizqie
Faculty of Computer Science
Universitas Sriwijaya
Palembang, Indonesia
qurhanul.rizqie@ilkom.unsri.ac.id

Iyus Maolana
Department of Radiology, Faculty of Medicine
Universitas Padjadjaran
Bandung, Indonesia

Eko Supriyanto
School of Biomedical Engineering and Health Sciences, Faculty of Engineering
Universiti Teknologi Malaysia
Johor, Malaysia

***Abstract*— Chest X-Ray is one of the most popular imaging modalities. Chest X-ray has been a subject of various imaging-related research for years. Among the various research, Lung segmentation is one of the most prominent ones. Nowadays the trend of research in segmentation is moving toward deep learning however traditional segmentation has advantage of requiring less calculation resources thus still has potential to be explored. In this paper an alternative non-deep learning segmentation method using graph-based method to trace border of the Chest X-Ray lung region is proposed. Chest X-Ray image was treated as a graph with coordinate of the pixels as vertex and value of the pixels as edges. First the image was divided into 4 quadrants, then the border of lung region on each quadrant was traced by finding the minimum spanning tree of the graphs on each quadrant, then the pixels recorded as the tree was smoothed and optimized using Savitzky-Golay filter. The results were analyzed using the confusion matrix by comparing the proposed method results with manual segmentation by a radiologist. The proposed method is successfully segment lung area on lateral view of chest X-Ray with an average accuracy of 0.936. Two sample T-test also employed in order to show that there is no significant difference between the proposed method results and manual segmentation by radiologist.**

Keywords— X-Ray, Lung Segmentation, Spanning Tree

I. INTRODUCTION

Chest X-ray Radiography (CXR) has been widely used as frequent screening in the detection, diagnosis, quantification, and treatment monitoring of many lung diseases [1-2]. Although Computed Tomography (CT) is endorsed as gold standard in lung examination, Chest X-Ray is still effective and practical for routine use due to very low radiation exposure, applicability in indicating abnormal formation in the lung, and widespread availability [3-4]. Furthermore, technological advancements in digital Chest X-Ray that enabled the obtaining of high quality image while maintaining radiation dose have emphasized its importance in radiology. With these great advantages, image analysis technologies in supporting Chest X-Ray are even now growing rapidly improving the diagnostic accuracy, ranging from enhancing the visibility, detecting and localizing abnormalities, to automated classification [4-6].

In lungs observation, the combination of two common views, frontal and lateral views, is applied as the standard practice in Chest X-Ray. In the frontal view, X-ray beam is directed through the front (anteroposterior/AP) or reversed (posteroanterior/PA) aspect of the chest in a standard distance in standing position [7]. AP position is easier to capture, especially in bedridden patients, however the interpretation is more difficult than that of PA position. In the lateral view, the X-ray beam is directed similar to that of frontal view, but the arm positioning needs to be managed in such a way that glenohumeral joint shadow has the least blockage in the Chest X-Ray [8].

As manual observation is the standard way in analysing Chest X-Ray, human factors, such as variability in expertise experiences and subjectivity, time consuming, and inter-observer variability, may cause inaccuracies. For this reason, the needs of automatic analysis in Chest X-Ray-based Computer-aided Diagnosis, are growing rapidly, not only supporting radiological works, but also generating numerous new information that manual observation cannot produce [9]. The segmentation process is one of the pre-processing needed before other processes can be applied. The segmentation process changes the representation of objects inside the image into something more suitable to analyse visually or computationally. In medical imaging, it was common for the segmentation process to be applied to images stacks. [9 - 12]

There are various methods and techniques developed for lung segmentation. The threshold method can be considered the simplest way to do a segmentation process [11]. Clustering or cluster analysis methods is an unsupervised image segmentation method [13]. On the more complex side, segmentation algorithms can be augmented by using artificial intelligence procedures, such as shape-based methods, classification methods, pattern recognition, fuzzy logic, neural networks, genetic algorithm approach, and deep learning [9,16-26].

Expansion of Souza method of ribs detection [14] to detect lung area on chest x-ray images is proposed. Souza presented an algorithm for automatic detection of posterior (dorsal) ribs in PA chest radiographs by taking vertical sections through the lung and determined rib edge points. In this process, he traced the outer edge of the lung to limit location of vertical section without the bottom and top edge. Pixels value in an image can be projected into a signal by the means of summation of the pixels in an area of the image. In the case of posterior chest x-ray, the projected signal would show two significant peak in the roughly centre of left and right lung objects.

This method is expanded by calculating the signature summation of the x-ray images on different area and use the minimum value of the pixels as starting point for line tracing algorithm. The tracing was done following a triangle like direction. From starting point the line is traced to above and below rows for inner and outer border, and left and right column for bottom border . This method captured the outer left, outer right, inner left, inner right and bottom border of the lungs.

II. EXPERIMENTAL SECTION

A. Chest X-Ray

Chest X-Ray images used in this experiment are collected from LIDC-IDRI. The Cancer Imaging Archive [15]. In this paper, the authors choose 30 Posterior-Anterior chest X-Ray images. The image is picked randomly with the only criteria is the image was clear enough to be manually segmented by an expert.

A radiologist is asked to draw lines around the edge of lung pleura and ribcage on the posterior-anterior view chest X-Ray image. These lines are treated as lung border and every pixel inside the border as the lung area. Later these area is used as the standard to be compared with the newly developed segmentation results

B. Lung Segmentation

The proposed method segmentation applied some principle based on graph theory, by treating the pixels as vertex, the detected borders of the lung can be described as a spanning tree of vertex. the inner border of each lung was taken as the starting value. Next, the outer edge was taken as the edge of the image from the left side and right side. After the section was defined, the tracing algorithm for the minimum spanning tree is applied. The initial tree vertex was located in the middle row of the radiograph and was then traced upwards and downwards one row at a time from this point. During tracing, the searching window was generated, which centre point is on the location of the vertex in the previous row. In upward tracing, the minimum spanning tree vertices was modified at each step to be the maximum of the computed vertex and the vertex on the previous row, reflecting the fact that the lung edge bent inwards towards the top, and also prevented it from being sidetracked when it meted the clavicle. A similar constraint cannot be applied to the downward tracing as the lung edge can bend both outwards and inwards in this direction.

After the minimum spanning tree for the outer edge of the lung is detected, the minimum spanning tree for the inner edge of the lung is also traced. Since the inner border of the lung is superimposed with the mediastinum, a clear inner border is hard to define. Using Sobel operators, a much clearer border can be defined. After the border is defined, then the minimum spanning tree process can be applied for the inner border. Right and left lungs have some notable differences in the term anatomy; for example, the left lung has two lung lobes, and the right lung has three lung lobes. The left lung is longer and smaller compared to the right lung, which means the right lung has a shorter and wider shape. The base of the left lung is closer to the heart than that of the right lung. The left lung has a solitary bronchus while the right lung has two. Projections of the left lung are isolated by oblique fissures, while a horizontal fissure isolates the right lung. The right lung is heavier than that of the left[33-40].

After the minimum spanning tree of the inner edge of the lung was detected, tracing window is applied to find the bottom edge of the lung. The initial vertex was estimated as a maximum of the intensities on the generated window from the bottom section at the left and right lung. Then, the minimum spanning tree of the bottom edge was traced right and left direction one column at a time from the initial vertex. The searching window is generated from the centre point on the vertex of the tree in the previous column. The visualization of the proposed algorithm can be seen in Figure 1.

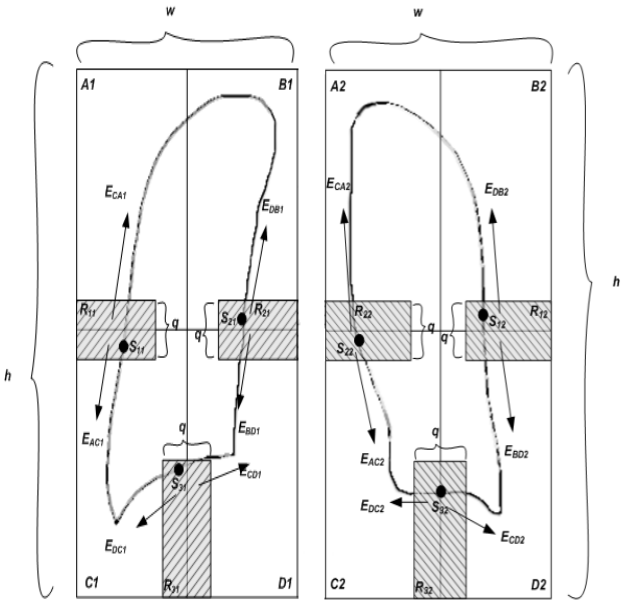

Fig 1. Quadrants of posterior-anterior view of lung on Chest X-Ray

First input image was pre-processed using histogram equalization in order to improve the quality of the image as well as normalize the images pixel range. Next the image was divided into 2 Region of Interest (ROI) for left and right lung, then for each area 4 quadrans A,B,C,D is initiated First, the image is divided into initial areas of R_{11}, R_{12}, R_{21}, R_{22}, R_{31}, and R_{32}. These initial areas are used to limit the area where the starting point of border tracing will be decided. In order to acquire the most optimum starting point, the areas must be near the outer, inner, and bottom border of the lung and roughly divided the lung into two parts. The initial area is decided as a percentage q of height h or width w of each ROI. The formula to define these areas can be written as follow :

$$R_{11} = (x,y); 0 < x < \frac{w}{4}; \frac{h}{2} - \frac{q}{2} < y < \frac{h}{2} + \frac{q}{2}$$

$$R_{12} = (x,y); 0 < x < \frac{w}{4}; \frac{h}{2} - \frac{q}{2} < y < \frac{h}{2} + \frac{q}{2}$$

$$R_{21} = (x,y); \frac{3w}{4} > x > w; \frac{h}{2} - \frac{q}{2} < y < \frac{h}{2} + \frac{q}{2}$$

$$R_{22} = (x,y); \frac{3w}{4} > x > w; \frac{h}{2} - \frac{q}{2} < y < \frac{h}{2} + \frac{q}{2}$$

$$R_{31} = (x,y); \frac{w}{2} - \frac{q}{2} > x > \frac{w}{2} + \frac{q}{2}; \frac{3h}{4} < y < h$$

$$R_{32} = (x,y); \frac{w}{2} - \frac{q}{2} > x > \frac{w}{2} + \frac{q}{2}; \frac{3h}{4} < y < h$$

From the stated initial area, the actual starting points for outer border of right and left lung S_{11} and S_{12} is chosen as the minimum pixels in the neighbourhood pixels of initial areas. For inner and bottom border tracing, in order to find the starting points, first the image will be processed into with Sobel operator, then the pixel with minimum value is chosen as the initial point S_{21} and S_{22} for inner border of right and left lung respectively, and S_{31} and S_{32} for bottom border of right and left lung respectively.

As stated above image *F(x,y)* was divided into four quadrants for each lung lobes for line tracing purposes. The division was based on the starting points, as described below

$$F_{A1}(x,y) = F(x,y);\ 0 < x < S_{31};\ 0 < y < S_{11}$$

$$F_{B1}(x,y) = F(x,y);\ 0 < x < S_{31};\ S_{21} < y < h$$

$$F_{C1}(x,y) = F(x,y);\ S_{31} < x < w;\ 0 < y < S_{11}$$

$$F_{D1}(x,y) = F(x,y);\ S_{31} < x < w;\ S_{21} < y < h$$

$$F_{A2}(x,y) = F(x,y);\ 0 < x < S_{32};\ 0 < y < S_{22}$$

$$F_{B2}(x,y) = F(x,y);\ 0 < x < S_{32};\ S_{12} < y < h$$

$$F_{C2}(x,y) = F(x,y);\ S_{32} < x < w;\ 0 < y < S_{22}$$

$$F_{D2}(x,y) = F(x,y);\ S_{32} < x < w;\ S_{12} < y < h$$

From the starting point, the next point in the upper, down, left or right direction is chosen, with the value of pixels is applied as the distance of the edges, *n* number of pixels are compared to find the minimum distance and the pixel with minimum distance was accepted as part of the detected edges. In Figure 2, a graph representation of pixels was presented. Sn was the starting point, and *V* was the vertex, and *E* was the edge. The graph was constructed based on pixels, and the vertex was synonymous with the coordinate of the pixels, while the edge was synonymous with the value of pixels. On figure 2, the lines with the arrow are the spanning tree of the graph. Meanwhile, the gray nodes were the candidate of the lung borders, and the black nodes were the selected node that detected as the lung border. The white nodes were the other unrelated pixels. Lets denote S_n as the starting vertex, and E_n as the minimum distance between the selected vertex and the next iteration. *n* value was chosen as a range of 5 based on observation, which results in the most optimal segmentation because the broader range might give erroneous smoothing.

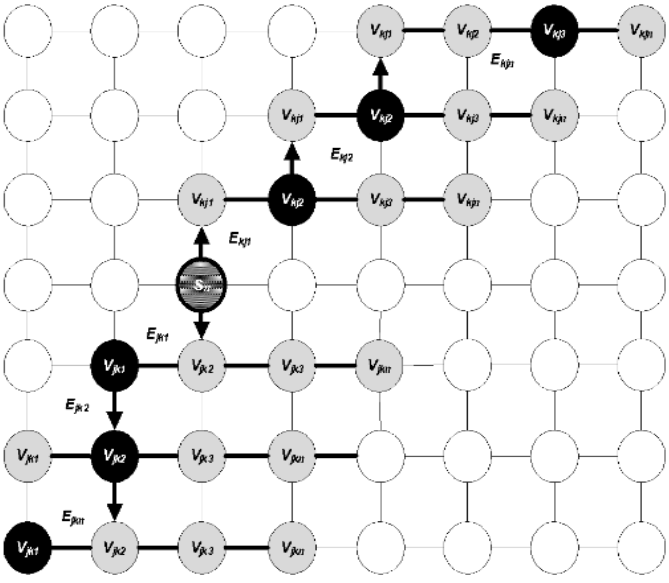

Fig 2. Graph representation of Pixels

In regards to Figure 3.5, E_{11} is the outer border of the right lung, which is the combination of traced border of E_{CA1} and E_{AC1}, with E_{CA1} is the border traced from S_{11} on the direction going from C_1 to A_1, and E_{AC1} is the border traced from S_{11} on the direction going from A_1 to C_1. Similarly E_{21} is the inner border of the right lung, which is the combination of traced border of E_{DB1} and E_{BD1}, with E_{DB1} is the border traced from S_{21} on the direction going from D_1 to B_1, and E_{BD1} is the border traced from S_{21} on the direction going from B_1 to D_1. The bottom border of right lung denoted E_{31} is the combination of traced border of E_{DC1} and E_{CD1}, with E_{DC1} is the border traced from S_{31} on the direction going from D_1 to C_1, and E_{CD1} is the border traced from S_{31} on the direction going from C_1 to D_1.

Meanwhile, E_{12} is the outer border of the left lung, which is the combination of traced border of E_{DB2} and E_{BD2}, with E_{DB2} is the border traced from S_{12} on the direction going from D_2 to B_2, and E_{BD2} is the border traced from S_{12} on the direction going from B_2 to D_2. Similarly E_{22} is the inner border of the left lung, which is the combination of traced border of E_{CA2} and E_{AC2}, with E_{CA2} is the border traced from S_{22} on the direction going from C_2 to A_2, and E_{AC2} is the border traced from S_{22} on the direction going from A_2 to C_2. The bottom border of right lung denoted E_{32} is the combination of traced border of E_{DC2} and E_{CD2}, with E_{DC2} is the border traced from S_{32} on the direction going from D_2 to C_2, and E_{CD2} is the border traced from S_{32} on the direction going from C_2 to D_2.

After outer, inner, and bottom border is detected for left and right lung. The results are smoothed using a border smoothing procedure. Finally, the detected border is integrated, and the lung area is extracted for both left and right lung. The result of the procedure is an image of the lung area as the foreground object and empty background. The flowchart for the proposed method is shown in figure 3.

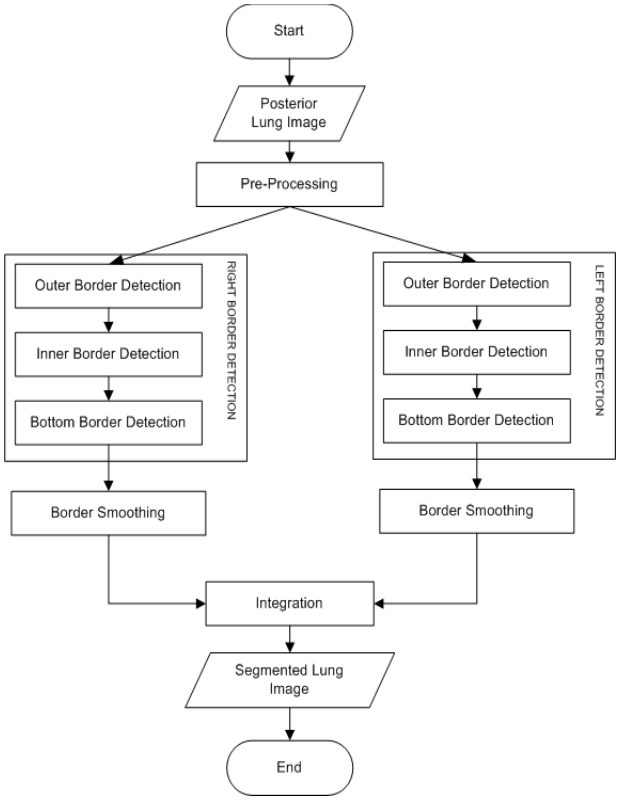

Fig 3. Lung Segmentation Flowchart

III. Results and Discussion

The result measured qualitatively and quantitatively, in order to measure quantitatively a gold standard provided by a radiology expert is compared with the results of the proposed algorithm. Chest X-Ray image used in this experiment is taken from LIDC-IDRI. The Cancer Imaging Archive (http://doi.org/10.7937/K9/TCIA.2015.LO9QL9SX). The experiments were conducted in a personal computer with Windows 8.1 operating systems, Intel i-5 processor, and 8GB RAM. The algorithm was developed on Matlab 2014a using image processing toolbox.

Figure 4 and 5 show the result of the segmentation process, Figure 4(a) show the histogram equalization results of input image, 4(b) show the detected starting point for outer side of left and right lung, starting point for inner side of left and right lung, and starting point for bottom side of left and right lung. 4(c) show the graph traced along the outer, inner, and bottom side of left and right lung, this graph the smoothed using Savitzky-Golay filter and the result is shown on 4(d). Lastly the area of left and right lung is extracted using the resulting graphs as guideline with the pixels inside detected borders are assigned as the area of lung, the results can be seen on figure 5.

The segmentation results are compared to the gold standard provided by a radiology expert. The expert manually segment lung area from lung Chest X-Ray images, then the results is used as a mask and compared to the proposed segmentation results. The process is shown on Figure 6. Pixels that is part of object segmented by both radiology expert and the proposed method is considered as True positive (TP), meanwhile pixels that segmented by the method but not by radiology expert is considered False Positive (FP). True negative (TN) is when pixels is detected as background by both radiology expert and the method, and finally False negative (FN) is when the method detect pixels as background but it was detected as object by the expert. Using this information accuracy of the proposed method can be calculated.

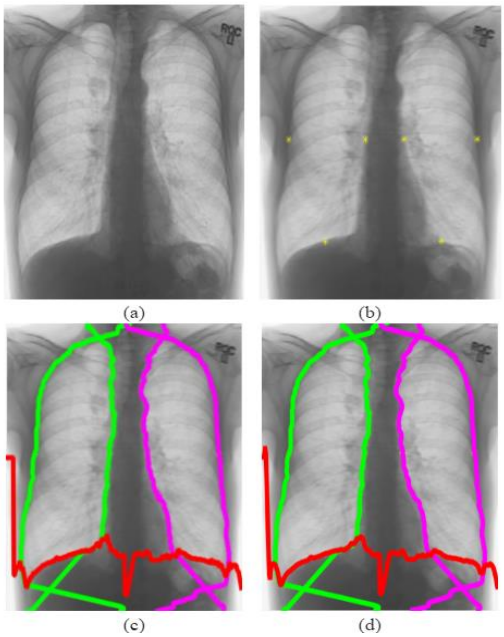

Fig 4. Image processing process from (a) Histogram Equalization (b) Border detection starting point (c) Border detected before smoothing procedure (d) Border detected after smoothing procedure

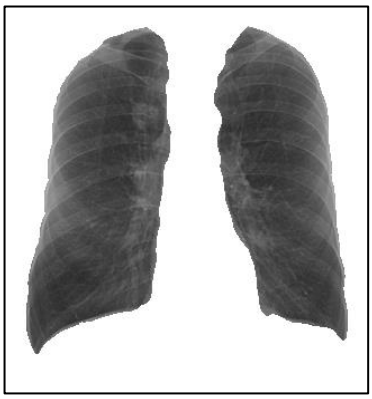

Fig 5. Extracted area of lung

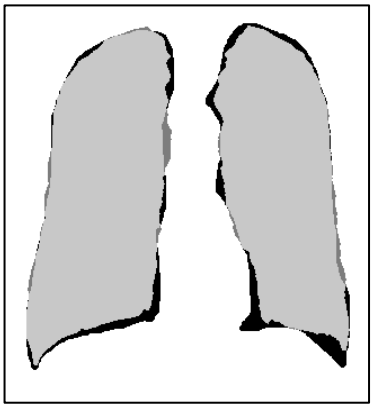

Fig 6 Comparison of segmentation result to manual segmentation

The proposed method emphasized the starting point of the traced graph and the initial area of R with height = q and width = $\frac{w}{4}$ for inner-outer border / posterior- anterior border and height = $\frac{h}{4}$ and width = q for the bottom border with q as the percentage of ROI height or width, w as the ROI width, and h as the ROI height. In the experiment for every X-Ray image, six different initial areas have experimented in order to find the best initial area that can be used to acquire the best starting point. The difference in the initial area depends on the percentage of q = [5, 10, 15, 20, 25, 30]. Various traditional and modern lung segmentation methods including machine learning and deep learning methods is used as comparison [19-26]. The results of the experiment can be seen on table 1.

Table 1. Comparison of accuracy of segmentation results

No	Algorithm	Accuracy
1	The proposed algorithm (R = 5)	0.9365
2	The proposed algorithm (R = 10)	0.936
3	The proposed algorithm (R = 15)	0.9365
4	The proposed algorithm (R = 20)	0.9335
5	The proposed algorithm (R = 25)	0.9285
6	The proposed algorithm (R = 30)	0.9195
18	Deep Neural Network [16]	0.9697
16	Deep Structured Learning [19]	0.948
17	CNN [20]	0.942
7	Region-based active contour method using prior shape and low-level features [21]	0.88
8	Edge Detection and Morphology [22]	0.8095
12	Low order adaptive region growing [23]	0.963
10	Hybrid ASM-PC [24]	0.934
11	Hybrid AAM-PC [24]	0.933
13	Fuzzy Curve [25]	0.927
14	ASM-SIFT [26]	0.920
15	ASM [26]	0.903

In the case of real data, it is harder to acquire the gold standard for comparison. While the confusion matrix can show how close the segmentation results of the proposed algorithm to radiology expert manual segmentation, it is not necessarily shown how close the segmentation results to the real objects. It is possible to have high accuracy but low precision by having segmented area that include all targeted area eventhough the shape is not similar. two-sample t-test is applied to the segmentation results in order to confirm that there is no significant difference between the proposed algorithm segmentation results compared to manual segmentation results by radiology experts. The alpha used in the test is 0.01, and the Pearson's Correlation (r) of the test results for the right side of the lung can be observed on table 2, and the Pearson's Correlation (P) of the test results for the left side of the lung can be observed on Table 3

Table 2 Pearson's Correlation (r) of the right lung region

q	r Region	r Eccentricity	r Orientation
5	0.33	0.07	0.96
10	0.38	0.20	0.91
15	0.38	0.21	0.92
20	0.47	0.28	0.71
25	0.35	0.49	0.44
30	0.35	0.42	0.51

Table 3 Pearson's Correlation (r) of the left lung region

q	r Region	r Eccentricity	r Orientation
5	0.28	0.77	0.35
10	0.29	0.70	0.50
15	0.29	0.95	0.56
20	0.30	0.97	0.60
25	0.45	0.67	0.44
30	0.53	0.49	0.38

The null hypothesis stated that there is no significant difference between region, eccentricity, and orientation of the lung regions segmented using the proposed algorithm and the lung region segmented manually by an expert. By comparing alpha with Pearson's Correlation (r) of the region, eccentricity, and orientation, a decision whether to accept or reject the null hypothesis can be made. In this research, it is decided that alpha= 0.01. From the table, it can be seen that all score of r for the region, eccentricity, and orientation in the right and left lung is higher than 0.01. The conclusion is that the null hypothesis is accepted for the region, eccentricity, and orientation on the right and left lung for every R.

IV. Conclusion

The modern trend of research about the segmentation of lung regions is moving toward the application of machine learning for the segmentation of lung regions. In this research an alternative approach for segmentation of lung regions is proposed. The proposed algorithm modifies a part of Souza[14] method for ribs detection and adds graph principle to the equation to create a triangle-shape based border tracing for lung regions. Graph theory is successfully applied to trace the border of lung area. The proposed method solve Souza method problem of never ended tracing by tracing from three different sides with each sides become the limit of the others side. The proposed method also improve Armato[15] method by simplify the calculation by divided the ROI into only 4 area. The methods show promising results based on accuracy. Compared to the conventional segmentation algorithm proposed method also has relatively higher accuracy. Unfortunately compared to machine learning based algorithms, the proposed algorithm still has less accuracy.

Acknowledgment

I acknowledge the National Cancer Institute and the Foundation for the National Institutes of Health, and their critical role in the creation of the free publicly available LIDC/IDRI Database used in this study

References

[1] B de Hoop B, C Schaefer-Prokop, H. A. Gietema, P. A. de Jong, B. van Ginneken, R. J. van Klaveren, M. Prokop. Radiology. Vol. 255(2), 629-637, 2010.

[2] J. Dworzak: 3-D Reconstruction of the Human Ribcage from 2-D Projection Images Using a Statistical Shape Model, (diploma thesis, Technische Universitat Berlin, 2009).

[3] M. Q. Rizqie, D. E. O. Dewi, M. A. Ayob, I. Maolana, R. Hermawan, R.D. Soetikno, E. Supriyanto. WSEAS Transactions on Biology and Biomedicine, Vol. 11(Art.#18), 133-139, 2014.

[4] J. Shiraishi, S. Katsuragawa, J. Ikezoe, T. Matsumoto, T. Kobayashi, K. Komatsu, M. Matsui, H. Fujita, Y. Kodera, K. Doi. AJR Am J Roentgenol. Vol. 174(1), 71-74, 2000.

[5] H. MacMahon, J. H. Austin, G. Gamsu. Radiology. Vol. 237, 395–400, 2005.

[6] T. Peters, K. Cleary, Image-Guided Interventions: Technology and Applications, Springer Science+Business Media, LLC (2008).

[7] B. van Ginneken, B. M. Ter Haar Romeny, Med. Phys. Vol. 27(10), 2445-2455, 2000.

[8] C. Wang, S. Guo, X. Wu, Bioinformatics and Biomedical Engineering, 3rd International Conference on, 1-4, 2009

[9] Agrawal S, Xaxa DK. Survey on image segmentation techniques and color models. International Journal of Computer Science and Information Technologies. 2014;5(3):3025-30.

[10] Russ JC. The Image Processing Handbook 2016 [Internet].

[11] Bankman I, editor. Handbook of medical image processing and analysis. Elsevier; 2008 Dec 24.

[12] Zaitoun NM, Aqel MJ. Survey on image segmentation techniques. Procedia Comput. Sci. 65, 797–806 (2015). International Conference on Communications, management, and Information technology (ICCMIT'2015).

[13] Chondro P, Yao CY, Ruan SJ, Chien LC. Low order adaptive region growing for lung segmentation on plain chest radiographs. Neurocomputing. 2018 Jan 31;275:1002-11.

[14] P. de Souza, Computer Vision Graphics and Image Processing, Vol. 23, 129-161, 1983.

[15] Armato III SG, McLennan G, Bidaut L, McNitt-Gray MF, Meyer CR, Reeves AP, Clarke LP. Data from lidc-idri. the cancer imaging archive. DOI http://doi. org/10.7937 K. 2015;9(7).

[16] Souza, Johnatan Carvalho, João Otávio Bandeira Diniz, Jonnison Lima Ferreira, Giovanni Lucca França Da Silva, Aristofanes Correa Silva, and Anselmo Cardoso de Paiva. "An automatic method for lung segmentation and reconstruction in chest X-ray using deep neural networks." Computer methods and programs in biomedicine 177 (2019): 285-296.

[17] Gaál, Gusztáv, Balázs Maga, and András Lukács. "Attention u-net based adversarial architectures for chest x-ray lung segmentation." arXiv preprint arXiv:2003.10304 (2020).

[18] Liu, Wufeng, Jiaxin Luo, Yan Yang, Wenlian Wang, Junkui Deng, and Liang Yu. "Automatic lung segmentation in chest X-ray images using improved U-Net." Scientific Reports 12, no. 1 (2022): 8649.

[19] Ngo, T. A. & Carneiro, G. Lung segmentation in chest radiographs using distance regularized level set and deep-structured learning and inference. In IEEE International Conference on Image Processing, 2140–2143. https://doi.org/10.1109/ICIP.2015.7351179 (2015).

[20] Rashid, R., Akram, M. U., Hassan, T. J. I. C. I. A. & Recognition. Fully convolutional neural network for lungs segmentation from chest X-rays. In International conference image analysis and recognition. https://doi.org/10.1007/978-3-319-93000-8_9 (2018).

[21] Saad MN, Muda Z, Ashaari NS, Hamid HA. Image segmentation for lung region in chest X-ray images using edge detection and morphology. In2014 IEEE International Conference on Control

System, Computing and Engineering (ICCSCE 2014) 2014 Nov 28 (pp. 46-51). IEEE.

[22] Annangi P, Thiruvenkadam S, Raja A, Xu H, Sun X, Mao L. A region based active contour method for x-ray lung segmentation using prior shape and low level features. In2010 IEEE international symposium on biomedical imaging: from nano to macro 2010 Apr 14 (pp. 892-895). IEEE.

[23] Chondro P, Yao CY, Ruan SJ, Chien LC. Low order adaptive region growing for lung segmentation on plain chest radiographs. Neurocomputing. 2018 Jan 31;275:1002-11.

[24] Van Ginneken B, Stegmann MB, Loog M. Segmentation of anatomical structures in chest radiographs using supervised methods: a comparative study on a public database. Medical image analysis. 2006 Feb 1;10(1):19-40.

[25] Coppini G, Miniati M, Monti S, Paterni M, Favilla R, Ferdeghini EM. A computer-aided diagnosis approach for emphysema recognition in chest radiography. Medical engineering & physics. 2013 Jan 1;35(1):63-73.

[26] Shi Y, Qi F, Xue Z, Chen L, Ito K, Matsuo H, Shen D. Segmenting lung fields in serial chest radiographs using both population-based and patient-specific shape statistics. IEEE Transactions on medical Imaging. 2008 Mar 31;27(4):481-94.